Supplementary data:

Figure S1

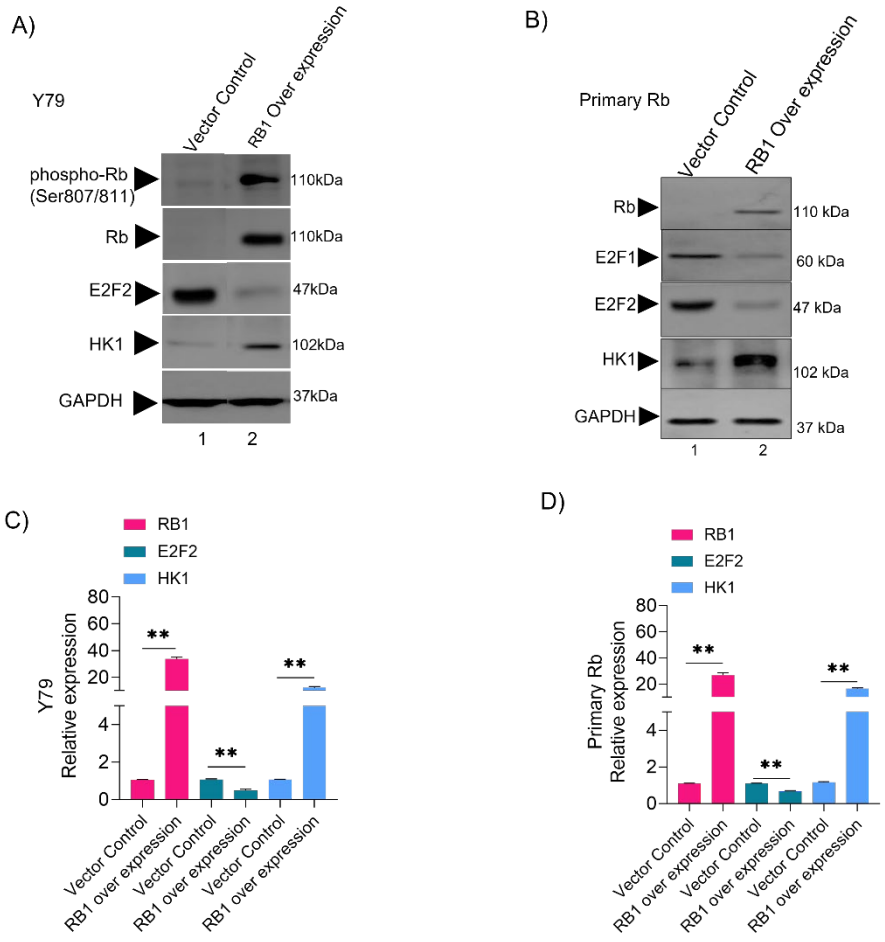

Figure S1. RB1 complementation induces HK1 and reduces E2F2 levels in-vitro. Western blot showing protein levels of Rb, phospho-Rb, E2F2 and HK1 in A) Y79 and B) GL1-Rb1. Gene expression of RB1, E2F2 & HK1 in control and RB1 complemented C) Y79 and D) GL1-Rb1 cells. . Values represent mean ± SEM. Unpaired two-sided Student's t-test was used for statistical analysis. *$p < 0.05$, **$p < 0.01$, ***$p < 0.001$, ****$p < 0.0001$.

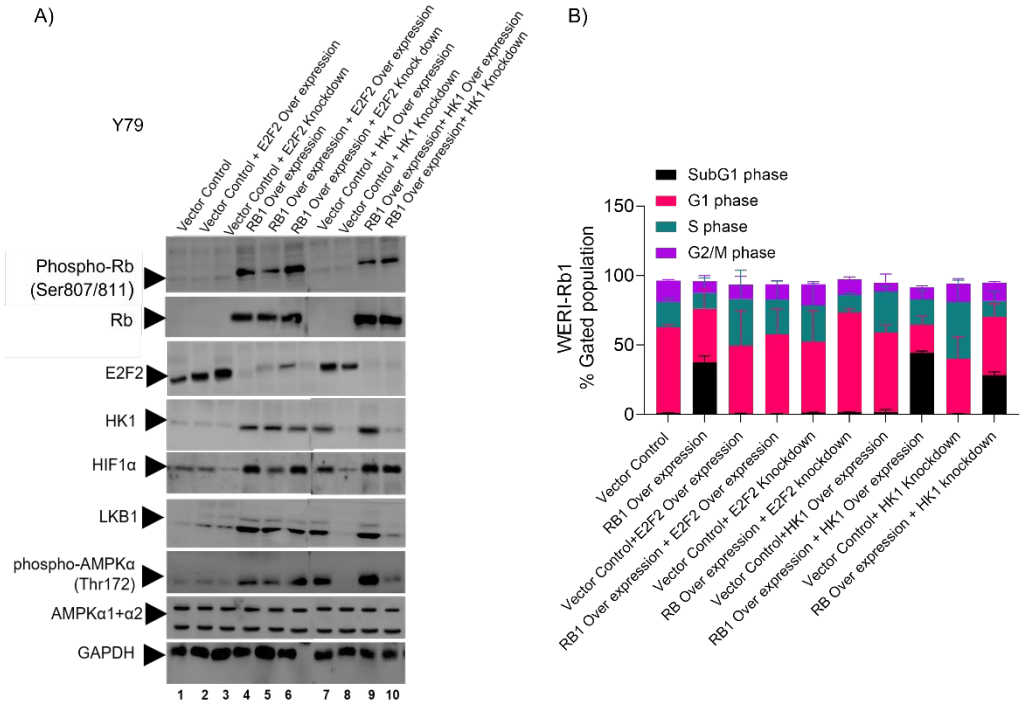

Figure S2. RB1 and HK1 uncover novel energy-sensing circuitry independent of canonical RB1-E2F2 cell cycle regulation. A) Western blot showing protein expression of candidate targets involved in energy sensing circuits and cell cycle in Y79. B) Cell cycle results showing percent gated cells in each phase of the cell cycle under RB1 overexpression compared to control (n=1, triplicate). *RB1* overexpression shows a high sub G1 cell population and cell cycle arrest at the G1/S phase. *HK1* overexpression shows no cell cycle arrest at the G1 phase and more cells gated at the S phase. *RB1* & *HK1* overexpression shows a high sub G1 population and less G1 cell population. *HK1* knockdown shows more distribution of cells in the S phase and G2/M phase (n=1, triplicate). *E2F2* overexpression condition shows more percent cells at S & G2/M phase. *RB1 & E2F2* overexpression shows a higher percentage of cells in the G1 phase, while the cell distribution in S & G2/M phase is reduced. *E2F2* knockdown shows higher cell distribution in the S phase and lower in the G2/M phase, while *E2F2* knockdown along with *RB1* overexpression shows less cell distribution in S & G2/M phase (n=1, triplicate).

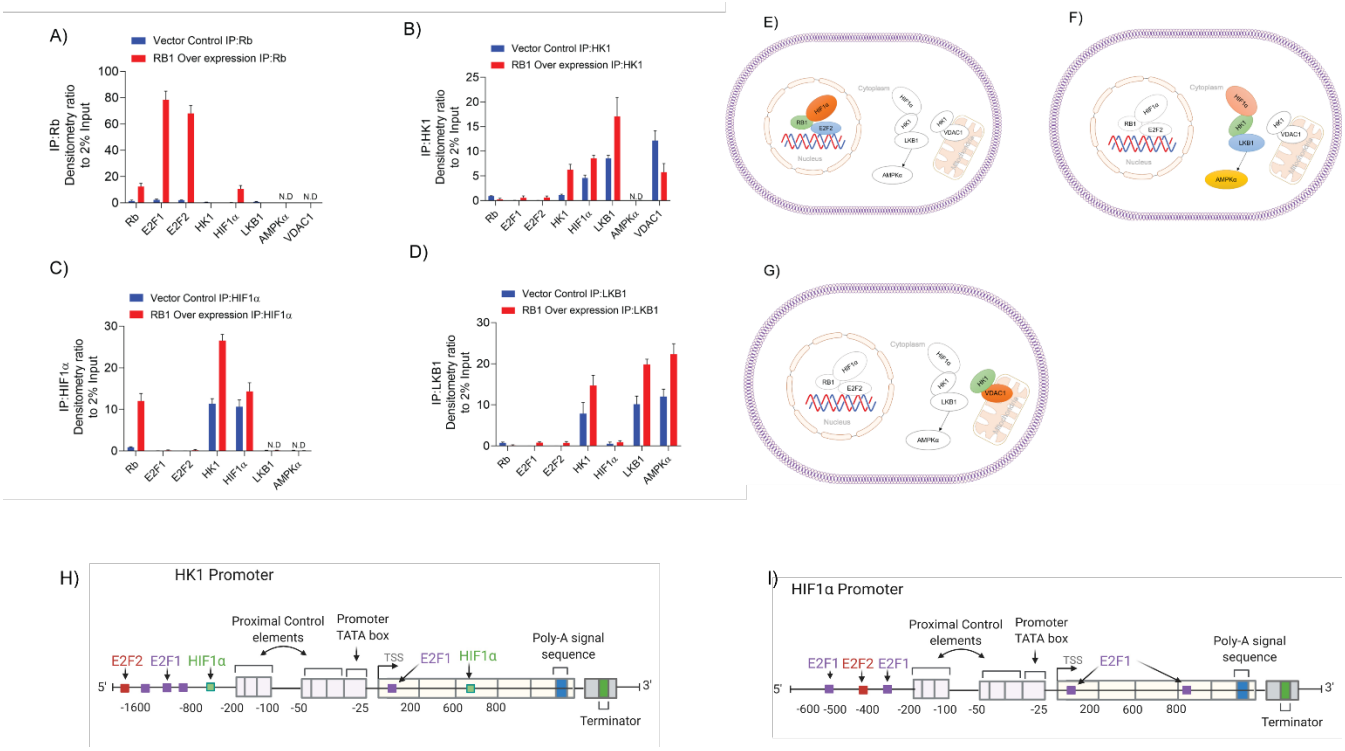

Figure S3. Interaction of RB with HIF1α and HK1 with LKB1 expedites metabolic changes in-vitro. A) Densitometry bar graphs showing Co-IP results having a ratio to 2% input of RB immunoprecipitation. Co-IP shows the interaction of RB with E2F1, E2F2 & HIF1α. B) Densitometry bar graphs showing Co-IP results having a ratio to 2% input of HK1 immunoprecipitation. Co-IP shows interaction with HIF1α, LKB1 and VDAC1. C) Densitometry bar graphs showing Co-IP results having ratio to 2% input of HIF1α immunoprecipitation. Co-IP shows interaction with RB and HK1. D) Densitometry bar graphs showing Co-IP results having a ratio to 2% input of LKB1 immunoprecipitation. Co-IP shows interaction with HK1 and AMPKα. E) Schematic representation of molecular players in the nuclear fraction. Nuclear fractions show the interaction of RB with HIF1α and E2F2. F) Schematic representation of molecular players in the cytoplasmic fraction. HK1 interacts with HIF1α and LKB1 in the cytoplasmic fraction. G) Schematic representation of molecular players in the mitochondrial fraction. HK1 interacts only with VDAC1 in the mitochondrial fraction. H) Schematic showing E2F1, E2F2 & HIF1α promoter binding sites in HK1 promoter. I) E2F1 & E2F2 binding sites in HIFα promoter. Promoter binding sites were analysed using the Eukaryotic Promoter Database (EPD).

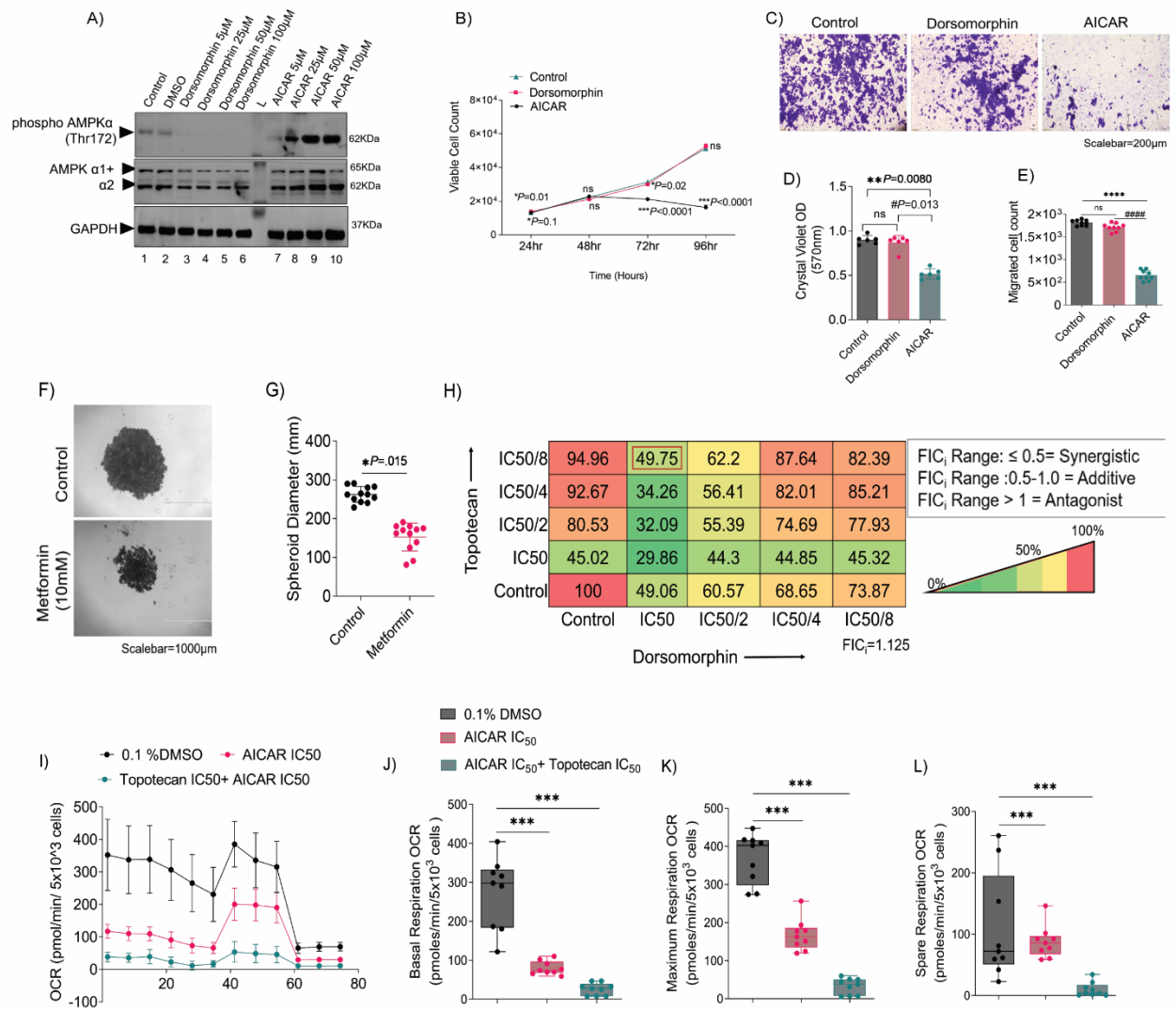

Figure S4: AMPKα activation halts cancer growth in-vitro and in-vivo A) Dose-dependent effects of AICAR and dorsomorphin on AMPKα activity. B) Cell viability assay to assess WERI-Rb1 cell proliferation under dorsomorphin and AICAR treatments for 96hours. C) Crystal violet staining of transwell insert membrane to assess D) Quantification of invasion of treated WERI-Rb1 cell groups. E) Migrated cells under dorsomorphin & AICAR treatments, evaluated by trypan blue assay in the transwell bottom chamber (n=3, triplicate). F) Tumor spheroids treated with an alternative AMPKα activator metformin(10mM) compared to control for 48hours. G) Scatter plot represents the area of tumor spheroids under metformin and AICAR treatment. H) Checkerboard assay to assess drug interactions between topotecan and dorsomorphin. I)Seahorse XFp Mito-stress assay to measure oxygen consumption rate (OCR) to assess mitochondrial function in WERI-Rb1 cells treated with 0.1 % DMSO (vehicle control), AICAR IC50, and their combination (n=3, triplicate). J) Basal respiration was reduced in combination therapy of AICAR IC50 & Topotecan IC50 compared to AICAR IC50 monotherapy and vehicle control conditions (0.1% DMSO). K) Maximum respiration was significantly reduced in combination therapy of AICAR IC50 & Topotecan IC50 compared to AICAR IC50 monotherapy and vehicle control conditions. L) Spare or reserve respiration was significantly reduced in combination therapy of AICAR IC50 & Topotecan IC50 compared to AICAR IC50 monotherapy and vehicle control conditions.

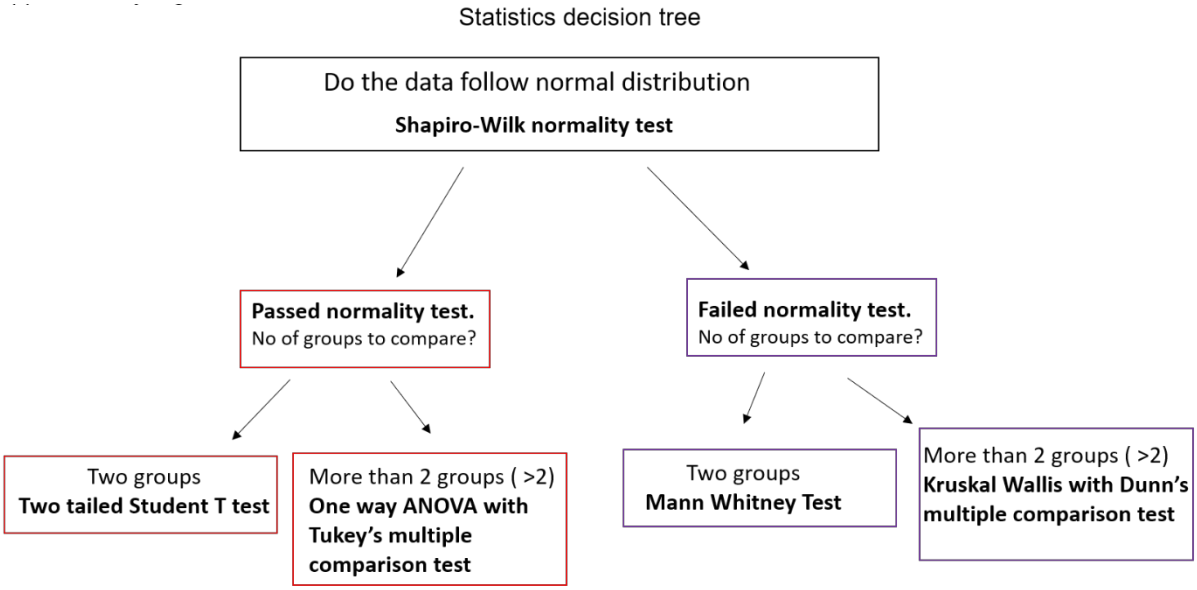

Figure S5: Statistical decision tree

Table S1: Details of the qPCR primers used for the study.

NCBI accession ID	Gene	Sense Primer	Length	Tm	Anti-sense Primer	Length	Tm
NM_000321	RB1	TTTGTAACGGGAGTCGGGA	19	58.2	CAGCGAGCTGTGGAGGAG	18	59.8
NM_004091	E2F2	GGTGAGGAGTGGATAAGG	18	59.9	AGAGGTCAGAAGTCAGAAG	19	59.6
NM_033500	HK1	CGTGTGCTGTTGATAATATCT	21	59.9	CTGTCAGGTGGTGTGATT	18	60.7
NM_001530	HIF1α	AGGAGGATCACCCTCTTCGT	20	58.63	TCTCCTCAGGTGGCTTGTC	19	57.4
NM_001101	βActin	TCCCTGGAGAAGAGCTACGA	20	57.9	AGGAAGGAAGGCTGGAAGAG	20	57.2

Table S2: Details of shRNA plasmids used for the study.

Plasmid	Cat#	Sequence	3'	5'	Loop
HK1 shRNA Rank1	ULTRA-3297147	TGCTGTTGACAGTGAGCGACTGCTACATGGAGGAGATGAAT AGTGAAGCCACAGATGTATTCATCTCCTCCATGTAGCAGGT GCCTACTGCCTCGGA	TTCATCTCCTCCATGTAGCAGG	ACTGCTACATGGAGGAGATGAA	TAGTGAAGCCACAGATGTA
HK1 shRNA Rank2	ULTRA-3297148	TGCTGTTGACAGTGAGCGATCCGATGAAACTCTCATAGAAT AGTGAAGCCACAGATGTATTCTATGAGAGTTTCATCGGAGT GCCTACTGCCTCGGA	TTCTATGAGAGTTTCATCGGAG	ATCCGATGAAACTCTCATAGAA	TAGTGAAGCCACAGATGTA
HK1 shRNA Rank2	ULTRA-3297150	TGCTGTTGACAGTGAGCGCCAAGGACAAGAAGTTACCTGAT AGTGAAGCCACAGATGTATCAGGTAACTTCTTGTCCTTGAT GCCTACTGCCTCGGA	TCAGGTAACTTCTTGTCCTTGA	CCAAGGACAAGAAGTTACCTGA	TAGTGAAGCCACAGATGTA
E2F2 shRNA Rank1	ULTRA-3231765	TGCTGTTGACAGTGAGCGACCCGGGGAGAAGACTCGGTATT AGTGAAGCCACAGATGTAATACCGAGTCTTCTCCCCGGGGT GCCTACTGCCTCGGA	ATACCGAGTCTTCTCCCCGGGG	ACCCGGGGAGAAGACTCGGTAT	TAGTGAAGCCACAGATGTA
E2F2 shRNA Rank2	ULTRA-3231766	TGCTGTTGACAGTGAGCGATGAGGACAACCTGCAGATATAT AGTGAAGCCACAGATGTATATATCTGCAGGTTGTCCTCAGT GCCTACTGCCTCGGA	TATATCTGCAGGTTGTCCTCAG	ATGAGGACAACCTGCAGATATA	TAGTGAAGCCACAGATGTA
E2F2 shRNA Rank3	ULTRA-3231767	TGCTGTTGACAGTGAGCGCCAGCGATCTCTTCGACTCCTAT AGTGAAGCCACAGATGTATAGGAGTCGAAGAGATCGCTGAT GCCTACTGCCTCGGA	TAGGAGTCGAAGAGATCGCTGA	CCAGCGATCTCTTCGACTCCTA	TAGTGAAGCCACAGATGTA
Non Target shRNA control	ULTRA-NT#4	TGCTGTTGACAGTGAGCGaaggcagaagtatgcaaagcatT AGTGAAGCCACAGATGTAatgctttgcatacttctgcctgT GCCTACTGCCTCGGA	atgctttgcatacttctgcctg	aaggcagaagtatgcaaagcat	TAGTGAAGCCACAGATGTA